RESEARCH DEPARTMENT

Image orthicon investigations: the measurement of currents within the tube

REPORT No. T-100

1963/2

THE BRITISH BROADCASTING CORPORATION
ENGINEERING DIVISION

RESEARCH DEPARTMENT

IMAGE ORTHICON INVESTIGATIONS: THE MEASUREMENT OF CURRENTS WITHIN THE TUBE

Report No. T-100

(1963/2)

C.R.G. Reed, M.A., A.M.I.E.E.
J.R. Sanders, M.A.

D. Maurice

(D. Maurice)

IMAGE ORTHICON INVESTIGATIONS: THE MEASUREMENT OF CURRENTS WITHIN THE TUBE

Report No. T-100

January 1963

(1963/2)

IMAGE ORTHICON INVESTIGATIONS: THE MEASUREMENT OF CURRENTS WITHIN THE TUBE

SUMMARY

This report describes investigations into certain aspects of the mechanism of signal production in the 4½ in image orthicon camera tube. The tube chosen was the type P822 (English Electric Valve Company Ltd.) since this tube is in general use at studio centres.

1. INTRODUCTION

Existing accounts of the image orthicon tube deal mainly with the 3 in version and less has been published about the 4½ in tube which, while similar in principle, has sufficient differences from the earlier tube to warrant separate investigation. The main objectives of the present work were, firstly, to devise techniques for measuring the currents flowing in the electrodes, and secondly to deduce from the results of such measurements the values of several important parameters of the tube. Earlier papers by D.C. Brothers[1] and F. Pilz[2] have described techniques for several measurements on image orthicon tubes which have served as very valuable starting points for the work described here. The data on the tubes supplied by the manufacturers have also been very valuable and some of their recommended working conditions are discussed in the light of the results of the measurements. Some investigations were also made into the effects of departures from the optimum conditions.

Some of the tube parameters, such as the sensitivity of the photocathode, can be measured directly with the tube operating in normal conditions. In other cases, it is necessary to make some change in the operating conditions or to make deductions from two or more sets of measurements, in order to measure such items as the beam current, the current gain of the secondary-emission multiplier, the transparency of the field mesh, the depth of modulation of the beam and the secondary-emission coefficient of the target when bombarded by the photo-electrons.

The experimental method which was adopted will be described in each case.

2. PRINCIPLES OF OPERATION OF THE IMAGE ORTHICON CAMERA TUBE

A brief description of the physical layout of the 4½ in image orthicon is given below, together with a simplified indication of the means whereby the camera tube produces an electrical signal which is related to the optical image of the scene.

TABLE 1

TYPICAL ELECTRODE POTENTIALS MEASURED WITH RESPECT TO CATHODE

Cathode	Earthed
Grid 1	-50 V to -100 V
Grid 2 (Dynode 1)	+300 V
Grid 3 (Persuader, Multiplier Focus)	+200 V to +300 V
Grid 4 (Wall Anode, Beam Focus)	+100 V to +200 V
Grid 5 (Decelerator)	+100 V to +250 V
Field Mesh	+15 V relative to G4
Target Mesh	Approximately cathode potential
Grid 6 (Image Accelerator)	40% to 80% of photocathode voltage (i.e. -160 V to -480 V)
Photocathode (Image Focus)	-400 V to -600 V
Magnetic focus field, at photocathode	0·012 Wb/m^2 (120 Gauss.)
Magnetic focus field, in scanning section	0·007 Wb/m^2 (70 Gauss.)

The complete tube is shown diagrammatically in Fig. 1. For the purposes of description it may conveniently be divided into three sections. These are:

(1) The image section

(2) The electron-gun and scanning section

(3) The multiplier section

2.1. The Image Section

The scene to be televised is focused on the photocathode (1), a semi-transparent layer of photoemissive silver/bismuth/caesium material deposited on the rear surface of the face plate (2). Light falling on the photocathode causes the emission of photo-electrons which are accelerated towards the target (3); the accelerating

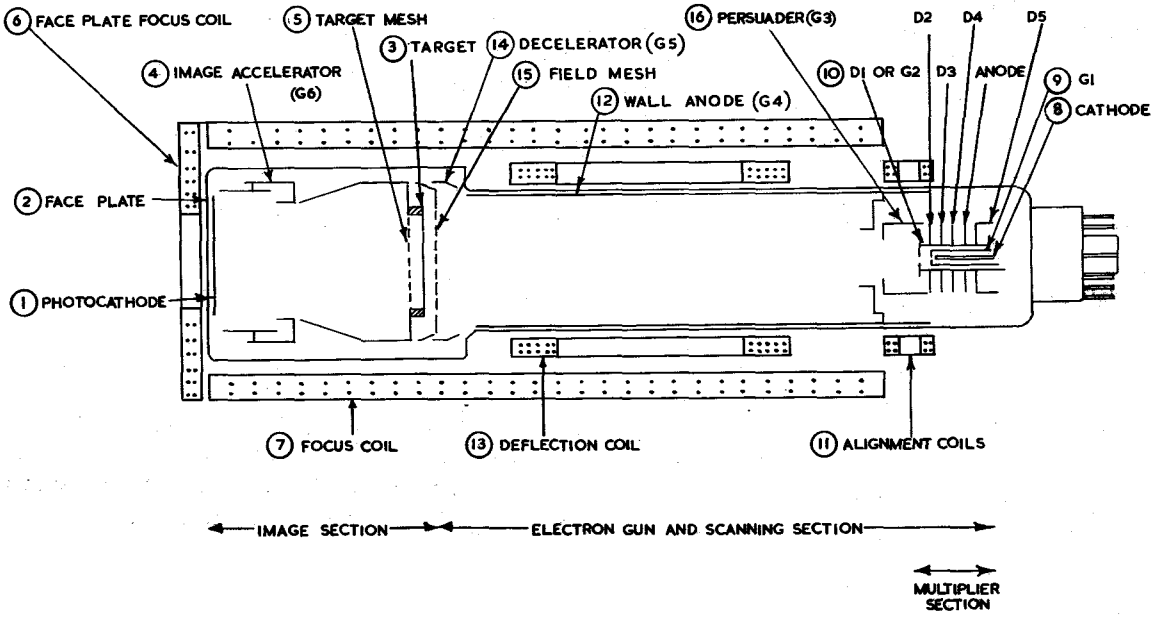

Fig. 1 - The $4\frac{1}{2}$" image orthicon (Schematic)

field is produced by the combined effects of the image accelerator (4) and the target mesh (5) which are held at potentials substantially positive with respect to the photocathode. The field is adequate to ensure saturated emission and therefore the number of electrons striking the target, per second, is proportional to the illumination at the photocathode. The target consists of a very thin glass disk and the fine metallic target mesh is placed very close and parallel to it. The photo-electrons are focused at the target by the longitudinal magnetic field produced by the face plate focus coil (6) and the main focus coil (7). On striking the target, with an energy of about five hundred electron volts, the photo-electrons produce secondary electrons, some of which are collected by the target mesh while others return to the target. Thus, there is a net loss of electrons from the mesh side of the target which results in the target acquiring a positive charge pattern representing the optical image at the photocathode.

2.2. The Electron-Gun and Scanning Section

The electron gun used to produce the scanning beam is of conventional design, with an indirectly heated cathode (8) surrounded by a control grid G1 (9). The anode of the gun (10) is termed grid 2 or dynode 1, and takes the form of a cylinder almost closed at one end. An extremely small aperture in the closed end emits a narrow beam of electrons that is used to scan the target. From G2 the beam passes through a transverse magnetic field produced by two small "saddle" coils (11) which are suitably placed in the scanning yoke and oriented to be at right angles to one another (these are the "alignment" coils). The field produced by these coils ensures that the beam from the gun enters the main focusing field parallel to its longitudinal axis. The electron beam is focused at the target by the combined action of the cylindrical electrode termed the wall anode (12), and the longitudinal magnetic field. Deflection is achieved by means of two pairs of "saddle" coils (13) (only one pair is shown in the diagram).

The decelerator G5 (14) can be varied in potential over a wide range, and serves to adjust the geometry of the field that exists between the wall anode and a fine mesh, termed the field mesh (15), which is held at a potential between 10 V and 30 V positive with respect to the wall anode. Since the target is stabilized near cathode potential by the target mesh, there is a decelerating field between it and the field mesh, which causes the beam electrons to approach the target at a low velocity.

The scanning beam will bring the rear surface of the target to an almost uniform potential, the greatest quantity of charge being accepted from the beam by those parts of the target that are most positive. Those electrons that do not land are accelerated back through the field mesh towards the electron gun. In this way the beam returning from the target becomes negatively modulated in amplitude by the picture information.

After an element of the target has been scanned two processes occur simultaneously. The positive and negative potentials on opposite faces of the target produce an electric field causing the flow of positive ions in the glass target; this removes most of the potential difference between the two surfaces before the element is scanned again. At the same time photo-electrons are bombarding the front surface of the target, building up a charge pattern which will be read off on the next scan.

2.3. The Multiplier Section

The beam returning from the target follows a path similar to that of the outgoing beam from the gun and it therefore lands on the outer surface of G2. This outer surface is the part of G2 known as dynode 1, and is coated with a secondary-emissive material. The electrons landing on D1 have an energy of approximately 300 electron volts, which is sufficient to produce several secondary electrons for every returning beam electron. Under the action of the field produced by the persuader G3 (16), the secondary electrons are guided into an electron multiplier consisting of D2, D3, D4, anode and D5, the output being taken from the anode. The electron multiplier provides a current gain of approximately 750. The normal signal-current output is approximately 15 μA.

3. ARRANGEMENT OF APPARATUS

For the investigations to be described, a standard camera channel was used, except for minor modifications made in order to facilitate the measurements. Monitoring of the output of the tube was carried out at a low impedance point at the output of the head amplifier, so that the signal could be observed before any form of signal processing had taken place.

A small panel was constructed into which the normal tube socket could be plugged and connections were made to a second tube socket which was fitted to the tube. The connections to the following electrodes were made through U-links on the panel:

(1) Cathode
(2) G1
(3) G2/D1
(4) Persuader (G3)
(5) Wall anode (G4)
(6) Multiplier final anode.

In addition, the connections to the field mesh and the decelerator were linked through the panel. The connections to the image section were reasonably accessible at plugs mounted on the yoke assembly.

A pulse generator was constructed in order to enable the potential of certain electrodes to be pulsed at line frequency, the pulse duration being variable between approximately 1·5 μs and 15 μs and the pulse amplitude being variable between zero and 70 V.

Many of the electrode currents were of the order 0·01 μA; for these measurements a mirror galvanometer having a deflection sensitivity of 400 mm/μA was used.

It was anticipated that, during the measurements, the signals from the tube might occasionally exceed their normal amplitudes, and therefore the head amplifier was checked with a test waveform input which exceeded the normal input by a factor of 10. There was no measurable non-linearity. The head amplifier voltage gain was measured with the aid of a voltage squarewave, having a period of 30 μs, fed into the test socket of the head amplifier.

4. THE MEASUREMENT OF WALL ANODE CURRENT

It was decided first to measure the current flowing to the wall anode. The possibility that this electrode might be collecting a small proportion of the beam current could not be overlooked, since an assumption that none of the beam was being collected would, if incorrect, render results of other measurements meaningless. The tube was exposed to an illuminated plain white surface and adjusted so that it was operating at half a lens stop above the "knee" of the transfer characteristic. The beam current was just adequate to discharge the target. The wall anode current was measured as a function of wall anode potential, all other electrode potentials being held constant. Table 2 shows the results of these measurements.

TABLE 2

WALL ANODE CURRENT

Cathode current (μA)	Wall anode potential (V)	Wall anode current (μA)
25·7	74·0	0·0025
25·7	96·0	0·0025
25·7	109·0	0·005
25·7	114·0	0·005
25·7	131·0	0·005
25·7	145·0	0·0063
25·7	158·0	0·0063
25·7	166·0	0·0075
25·7	178·0	0·0075

Measurements were repeated with the lens capped and then with the cathode current at zero. In neither case was there any measurable change in the above readings. The current was also unaffected by changing other electrode potentials.

Since the measured current is dependent upon the wall anode voltage only, it is assumed that it is caused by leakage in the tube and its connections.

It would appear that none of the scanning beam reaches the wall anode under normal conditions.

5. THE MEASUREMENT OF BEAM CURRENT

A simple and reliable method of measuring the beam current is necessary since the magnitude of the beam current affects the discharge of the target and contributes to the noise in the final output; it is also necessary to know the beam current in order to determine the gain of the multiplier section.

It was found that the beam current is most conveniently measured by using one or more electrodes as collectors, the main problems being the choice of suitable electrodes and the need to separate the required current from other currents which may flow. Difficulties may arise caused by leakage currents in the tube and its connections or by secondary emission at the collecting electrodes.

The field mesh is not suitable for collecting the beam; it is approximately 70% transparent and most of the beam will pass through. The target and target mesh are also unsuitable because their currents are affected by the emission from the photocathode. The most convenient electrodes are the wall anode (G4) and persuader (G3).

Two different approaches to the problem were tried, and details of both are given in the following sections. Although the first method used proved unsuccessful, the results obtained are included because they illustrate the difficulties of making such measurements.

The current measurements were made with the mirror galvanometer already mentioned (deflection sensitivity 400 mm/μA).

5.1. The First Method used for the Measurement of Beam Current

The wall anode and persuader were connected together and made positive with respect to the gun anode D1. The field mesh and decelerator were earthed; a subsidiary measurement showed no current to either electrode provided that the wall anode was held more than 20 V positive with respect to D1. The scan generators were made inoperative and the multiplier action stopped by removing the 1·2 kV e.h.t. from the dynode chain. The target mesh was biased negatively by about 4 V in order to prevent the collection of electrons by the target, and the focus coil current held at its normal value.

Direct current was then passed through the line scan coils in order to deflect the beam towards the wall anode.

The potential of the wall anode and persuader was varied and their combined current measured for several different values of direct current in the line scan coils. Graphs of three sets of results are shown in Fig. 2. It was found that the shapes of the curves varied violently with small changes in the direct current, particularly when this exceeded 0·6 A, and also that they depended upon the setting of the vertical shift control of the camera. In order to explain the peaks and troughs of the curves, the currents to the wall anode, persuader, D2 and D3 were measured separately and it was found that each contained peaks and troughs as shown in Fig. 3. An attempt was made to find similar effects at D1, but the small beam current could not be measured in the presence of the much larger current collected by the electrode in its role as the anode of the electron gun.

The deficiencies of this method are mainly due to the return of the beam to the dynode system, with the consequent release of secondary electrons, instead of the intended collection by the wall anode or persuader. The electrostatic field resulting from low voltages at the decelerator and field mesh reflects the beam, and the magnetic field of the focus coil then tends to make it travel back towards the dynodes.

In this experiment the tube was being operated under conditions which were far from normal and the return beam was probably not falling on D1 but was reaching instead the multiplier chain D2, D3, etc. (A similar effect occurs with

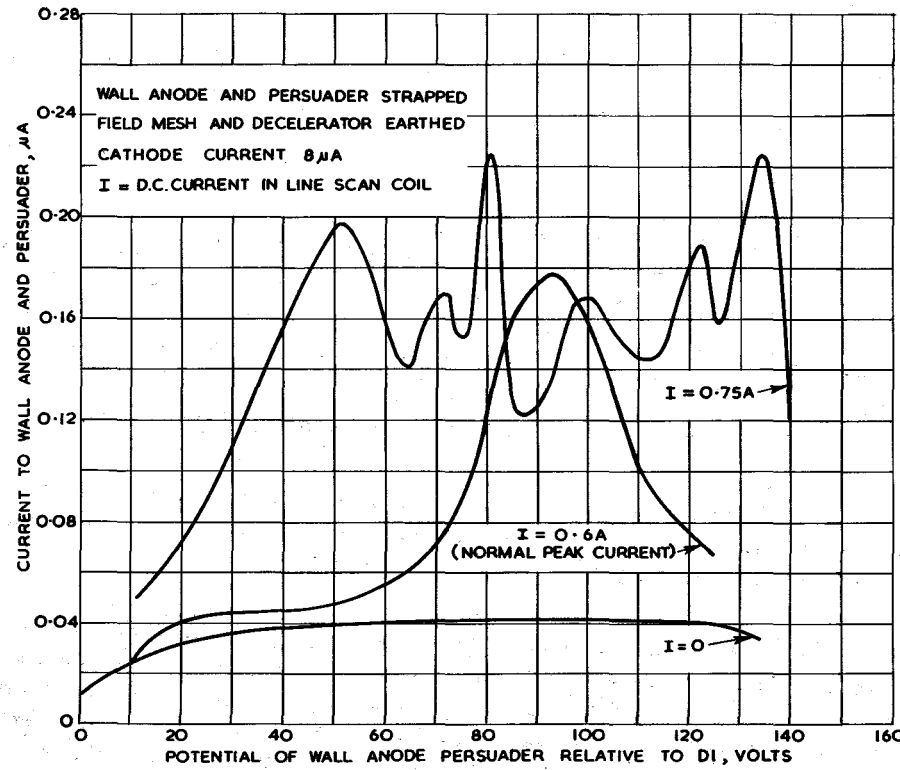

Fig. 2 - Wall anode and persuader currents measured during the determination of beam current (method 1)

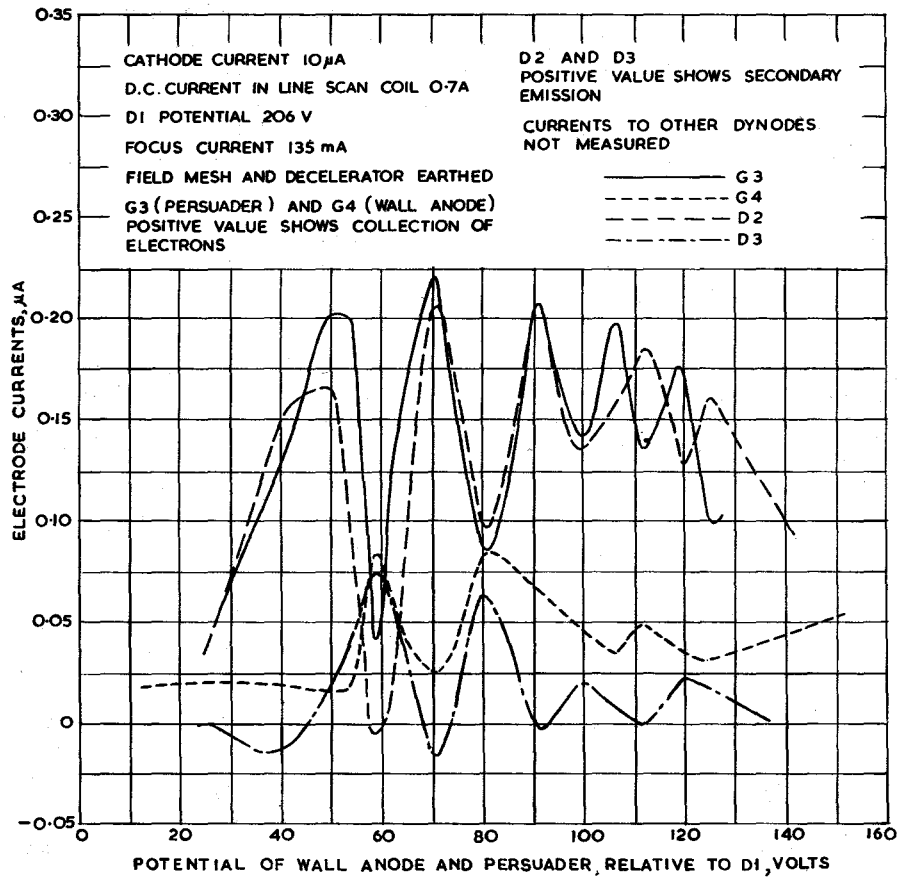

Fig. 3 - Electrode currents obtained during the measurement of beam current (method I)

normal scans and persuader voltage if the field mesh is less positive than the wall anode; this results in an image of D1 and D2 on the picture monitor.) Small variations in any of the operating conditions can make the beam return to a different part of the dynode system and cause severe changes in the secondary emission from the dynodes and the collection of electrons by the persuader and wall anode.

5.2. The Second Method used for the Measurement of Beam Current

The channel was set up in a similar manner to that used for the first method except that the beam was de-focused by switching off the focus current and the current in the scanning coils was also removed.

The field mesh and decelerator were first connected to earth through the galvanometer, and the target mesh biased to 4 V negative with respect to cathode: the measured current was found to be negligibly small. The galvanometer was then re-connected in order to measure the combined wall anode and persuader currents, the field mesh and decelerator being taken directly to earth. The tube was thus operating under conditions which were very far from normal but some justification for the use of this method will be shown later.

The combined current flowing in wall anode and persuader was measured with:

(i) the cathode current set to a known value,

(ii) G1 biased very negatively, in order to cut off the beam current.

The difference between the two readings was taken as the value of the beam current. Readings were taken with the wall anode and persuader positive to D1 by:

(a) 80 V
(b) 140 V
(c) 200 V

The results are shown in Table 3.

TABLE 3

BEAM CURRENT I_B AT THREE SETTINGS OF WALL ANODE AND PERSUADER POTENTIAL (V)

Cathode current μA	V = 80 V $I_B \cdot \mu A$	V = 140 V $I_B \cdot \mu A$	V = 200 V $I_B \cdot \mu A$	Mean $I_B \cdot \mu A$
0	0	0	0	0
5	0·0212	0·0188	0·0200	0·0200
10	0·0425	0·0388	0·0413	0·0407
15	0·0600	0·0575	0·0588	0·0588
20	0·0750	0·0725	0·0750	0·0742
25	0·0900	0·0875	0·0889	0·0881
30	0·105	0·100	0·103	0·103
40	0·130	0·128	0·130	0·129
50	0·158	0·153	0·155	0·155
60	0·184	0·180	0·183	0·182
70	0·211	0·208	0·208	0·209
80	0·234	0·235	0·236	0·235
90	0·266	0·263	0·265	0·265
100	0·296	0·291	0·295	0·294

Within the limits of measurement, the beam current collected is independent of the voltage applied to the wall anode and persuader, i.e. it is probable that all the current was collected by these electrodes. The result is shown graphically in Fig. 4.

The line and field scan currents were then restored and normal e.h.t. was applied to the multiplier section of the tube; the focus current, however, remained disconnected. The multiplier anode current was then measured and found to be less than 1 μA, compared with about 100 μA obtained under normal working conditions with a cathode current of 100 μA, indicating that virtually all the beam was being collected by the wall anode and persuader and had not returned to the multiplier. Other electrodes could be ruled out, since previous measurement had shown that the field mesh and decelerator were not collecting current, and the target was not collecting because of the bias on the target mesh. It would appear, therefore, that the result given by the second method of measurement was a true assessment of the current in the beam.

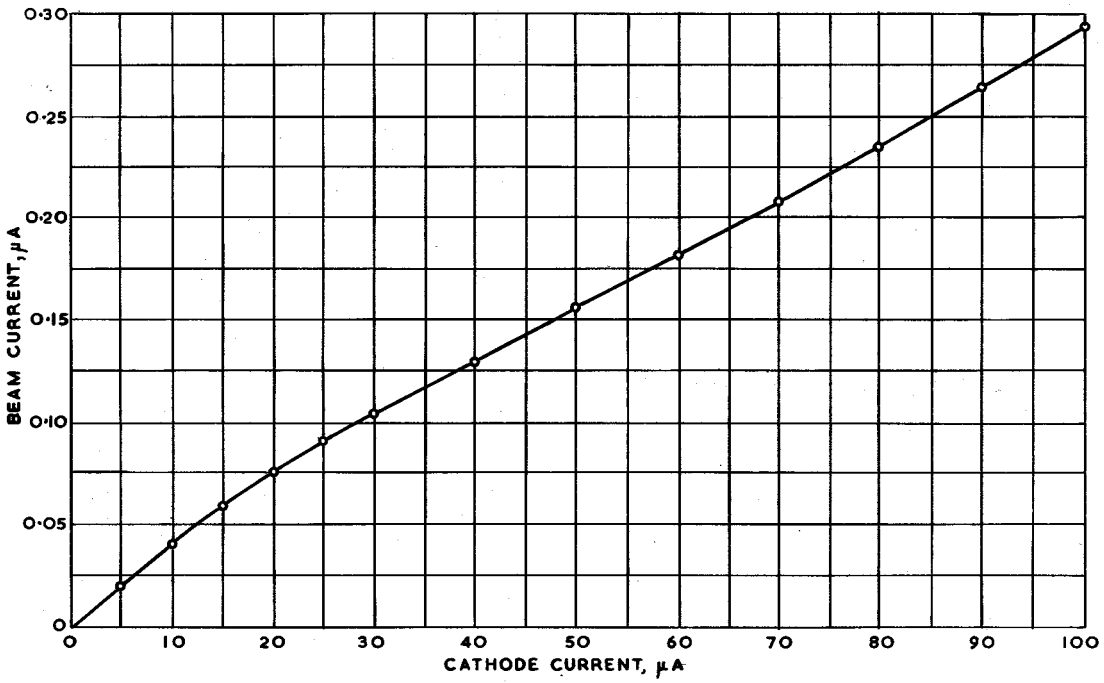

Fig. 4 - The relationship between beam current and cathode current

It is possible that secondary electrons from the edge of the hole in D1 contribute to the measured beam current but do not form part of the useful beam under normal operating conditions. This effect is thought to be very small, a view which is supported by the results of Section 6 of this report where the transparency of the field mesh to the electron beam, deduced from the measured beam current, is found to be in close agreement with its known optical transparency.

The results obtained for the two methods used show that the main difficulty in measuring the beam current lies in collecting the current without, at the same time, introducing errors caused by secondary emission, and that this problem is very much simplified by removing the axial magnetic focusing field. While the first attempt at measurement was unsuccessful, it illustrated some aspects of the operating mechanism of the tube.

6. THE MEASUREMENT OF FIELD-MESH TRANSPARENCY

The optical transparency of the field mesh was known to be approximately 70%. It was, however, considered desirable to measure its transparency to the electron scanning beam. The transparency, T, of the field mesh, is defined as the ratio of the current not collected by the field mesh (in one transit of the beam through the mesh) to the total current approaching the mesh. Let the incident-beam current be I_B, then the mesh absorbs $(1 - T)I_B$ and transmits TI_B at the first passage of the beam through the mesh. If the returning beam current is TI_B, i.e., all the beam returns from the target, the mesh absorbs $(1 - T)TI_B$ and transmits T^2I_B.

Thus the total field-mesh current,

$$I_F = (1 - T^2)I_B$$

whence $$T = (1 - I_F/I_B)^{\frac{1}{2}}$$

Since the incident beam current is known as a function of the cathode current, (see Table 3), the transparency of the field mesh can be calculated from measurements of the cathode and field-mesh currents.

The following electrode potentials were used during the measurements:

Target mesh:	−3·0 V	with respect to cathode
Field mesh:	+149 V	with respect to cathode
Wall anode:	+130 V	with respect to cathode
Decelerator:	0 V	with respect to cathode

It will be seen that the field mesh was maintained 19 V above the wall anode potential; this is a normal operating condition. The target mesh potential of −3·0 V ensured that all the beam electrons were reflected by the target.

The field-mesh current was measured at different cathode currents; the results of the measurements together with the derived values of T are shown in Table 4.

TABLE 4

THE "ELECTRON" TRANSPARENCY OF THE FIELD MESH

Cathode current μA	Beam current (I_B) μA	Field-mesh current (I_F) μA	Proportion of beam current collected by field mesh (I_F/I_B)	Proportion of beam current transmitted by field mesh ($1 - I_F/I_B$)	T
10·0	0·041	0·021	0·51	0·49	0·70
20·0	0·074	0·038	0·51	0·49	0·70
30·0	0·103	0·052	0·50	0·50	0·71
40·0	0·129	0·066	0·51	0·49	0·70
50·0	0·155	0·077	0·50	0·50	0·71

It will be seen that the value of "electron" transparency obtained is in good agreement with the value obtained optically.

This figure of 0·7 for the "electron" transparency of the field mesh can be expected under normal operating conditions. Under less conventional conditions there can be an apparent change from this figure. This is investigated in the following section.

7. THE MEASUREMENT OF SECONDARY EMISSION FROM THE FIELD MESH

It was found that when the field mesh was more than 18 V positive with respect to the wall anode, the field mesh current was virtually independent of the decelerator voltage. With smaller differences between the field mesh and wall anode potentials the field mesh current was found to be dependent upon the decelerator potential.

This effect might be anticipated, since the decelerator voltage affects the potential gradient on the cathode side of the field mesh; both axial and radial electrostatic field components are produced. The axial components of this field determine whether secondary electrons produced by the scanning beam at the field mesh will return to the mesh or travel to D1. It will be appreciated that the escape of secondary electrons from the field mesh will cause an apparent change in the "electron" transparency of the mesh, the "electron" transparency being defined as in Section 6. Since the axial component is not uniform over the surface of the field mesh, the production of secondary electrons can be expected to produce shading signals. The effect of varying the potential between the field mesh and the wall anode was investigated for two widely different decelerator potentials.

The results of these measurements where the decelerator was negative with respect to the field mesh are shown in Table 5. The tube electrode potentials were:

Decelerator:	−100 V with respect to cathode
Wall Anode:	+132 V with respect to cathode
Cathode Current:	10·0 μA (Beam current I_B = 0·041 μA)

TABLE 5

VARIATION OF "ELECTRON" TRANSPARENCY OF FIELD MESH AS A FUNCTION OF FIELD MESH POTENTIAL

Field-mesh potential with respect to wall anode	Field-mesh current (I_F)	Proportion of beam current collected (I_F/I_B)	Proportion of beam current transmitted ($1 - I_F/I_B$)	T
V	μA			
1·1	0·019	0·46	0·54	0·74
2·3	0·019	0·46	0·54	0·74
3·7	0·020	0·49	0·51	0·71
5·2	0·020	0·49	0·51	0·71
10·6	0·020	0·49	0·51	0·71
14·9	0·020	0·49	0·51	0·71
19·6	0·021	0·53	0·47	0·69
26·9	0·021	0·53	0·47	0·69
34·9	0·022	0·55	0·45	0·67
45·0	0·021	0·53	0·47	0·69

It will be seen that in these conditions the apparent transparency varies very little. It may, therefore, be concluded that few secondary electrons escape from the field mesh.

The decelerator was then made positive with respect to the field mesh and a similar set of measurements was made. The results of these measurements are shown in Table 6. The tube electrode potentials were:

Decelerator:	+210 V with respect to cathode
Wall anode:	+132 V with respect to cathode
Cathode current:	10·0 μA (Beam Current I_B = 0·041 μA)

TABLE 6

VARIATION OF "ELECTRON" TRANSPARENCY OF FIELD MESH AS A FUNCTION OF FIELD MESH POTENTIAL

Field-mesh potential with respect to wall anode	Field-mesh current (I_F)	Proportion of beam current collected (I_F/I_B)	Proportion of beam current transmitted ($1 - I_F/I_B$)	T
V	μA			
0·5	−0·0013	−0·032	1·032	1·02
1·5	0·0063	0·15	0·85	0·92
2·4	0·010	0·24	0·76	0·87
3·6	0·013	0·32	0·68	0·83
5·0	0·015	0·37	0·63	0·79
10·0	0·018	0·44	0·56	0·75
15·0	0·019	0·46	0·54	0·73
20·0	0·021	0·51	0·49	0·70
25·0	0·021	0·51	0·49	0·70
30·0	0·021	0·51	0·49	0·70
35·0	0·021	0·51	0·49	0·70
40·0	0·022	0·54	0·46	0·68
45·0	0·022	0·54	0·46	0·68

The results given in Tables 5 and 6 are shown graphically in Fig. 5.

In the case of a decelerator potential of +210 V, it will be seen that when the field mesh is less than approximately 15 V positive with respect to the wall anode, there is considerable secondary emission from the field mesh which adds to the beam returning to D1. This secondary emission will cause shading signals to appear in the tube output, since the escape of secondary electrons will not be uniform over the whole area of the field mesh. Another undesirable effect of the dilution of the return beam by secondary electrons is that they will contribute additional noise to the output of the tube and hence the signal-to-noise ratio will be impaired.[1]

The conclusion which may be drawn from these measurements is that the field mesh must be maintained at least 15 V positive with respect to the wall anode if the decelerator potential is to be adjustable over a wide range.

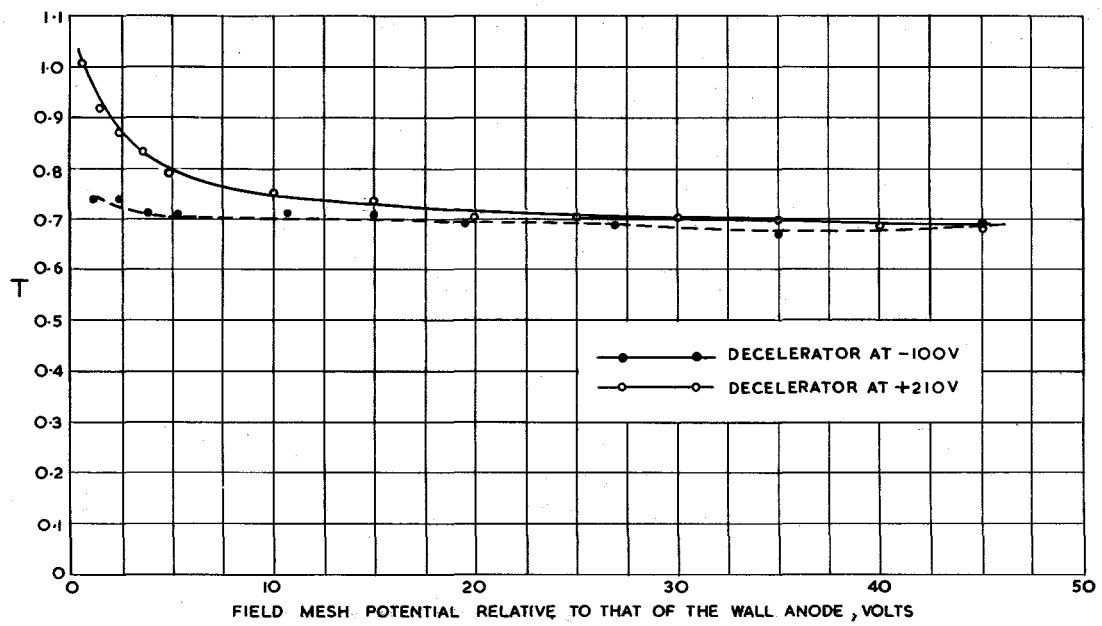

Fig. 5 - The variation of the effective transparency of the field mesh as a function of field mesh potential

8. THE MEASUREMENT OF OUTPUT AND SHADING AS A FUNCTION OF PERSUADER VOLTAGE

The persuader voltage is normally adjusted to give maximum signal output consistent with minimum shading. Measurements were made to determine how closely the condition for maximum output corresponded with the condition for minimum shading.

An output signal was created by applying negative going pulses to G1 in order to cut off the beam for approximately 8 μs during each line scan; the cathode current was maintained at a fixed value, so that the picture signal component of the beam returning to D1 was maintained constant. Measurement of the pulse amplitude at the tube output as a function of persuader voltage then provided a measurement of the variation of picture signal output as a function of persuader voltage. The lens was capped during these measurements.

Shading was measured as the maximum voltage excursion from the base of the pulse, along a line at the centre of the picture; the shading was considered to be positive when in the same direction as the pulse, and negative when in the opposite direction. This convention is shown in Fig. 6 for the case of "bend" type shading. This is the predominant type of shading observed, but over a limited region the waveform is irregular.

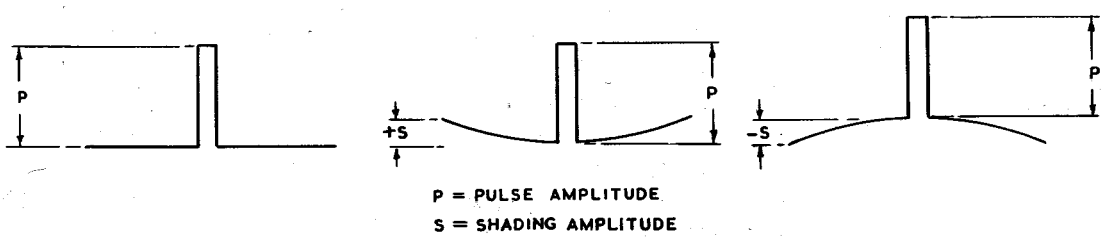

Fig. 6 - Conventions used to define shading signals

All electrode potentials, with the exception of that of the persuader, were held constant. These were as follows:

Target mesh:	−3·0 V with respect to cathode
Wall anode:	+111 V with respect to cathode
Field mesh:	+126 V with respect to cathode
Decelerator:	−100 V with respect to cathode
1st Dynode:	+220 V with respect to cathode
Cathode current:	10·0 μA

Table 7 shows the results of these measurements.

TABLE 7

EFFECT OF PERSUADER POTENTIAL ON OUTPUT

Persuader potential	Pulse amplitude	Shading amplitude	
V	V	V	
161	0·063	+0·012	
176	0·088	+0·015	
190	0·120	+0·010	
204	0·140	+0·005	
219	0·145	0	
236	0·135	−0·005	
248	0·105	−0·010	
250	0·106	−0·005	In this region the shading was no longer a simple "bend", but was irregular in shape.
255	0·121	−0·005	
265	0·131	−0·015	
280	0·126	−0·010	
294	0·108	−0·010	
309	0·096	−0·011	
325	0·090	−0·015	
344	0·083	−0·024	

These results are shown graphically in Fig. 7. It may be concluded from this result that a condition for maximum signal output with minimum shading may be found but care must be exercised, since more than one peak of output signal level may be encountered, only one of which will coincide with minimum shading.

9. THE MEASUREMENT OF GAIN OF THE MULTIPLIER SECTION

The current gain of the multiplier section of this type of tube is quoted as being between 500 and 1000; it was therefore considered worth while to check this figure. Two methods were used.

9.1. The First Method Used to Determine Multiplier Gain

Negative-going line frequency pulses of 6 μs duration were applied to G1, cutting off the beam during the pulse. The cathode current was measured, and from

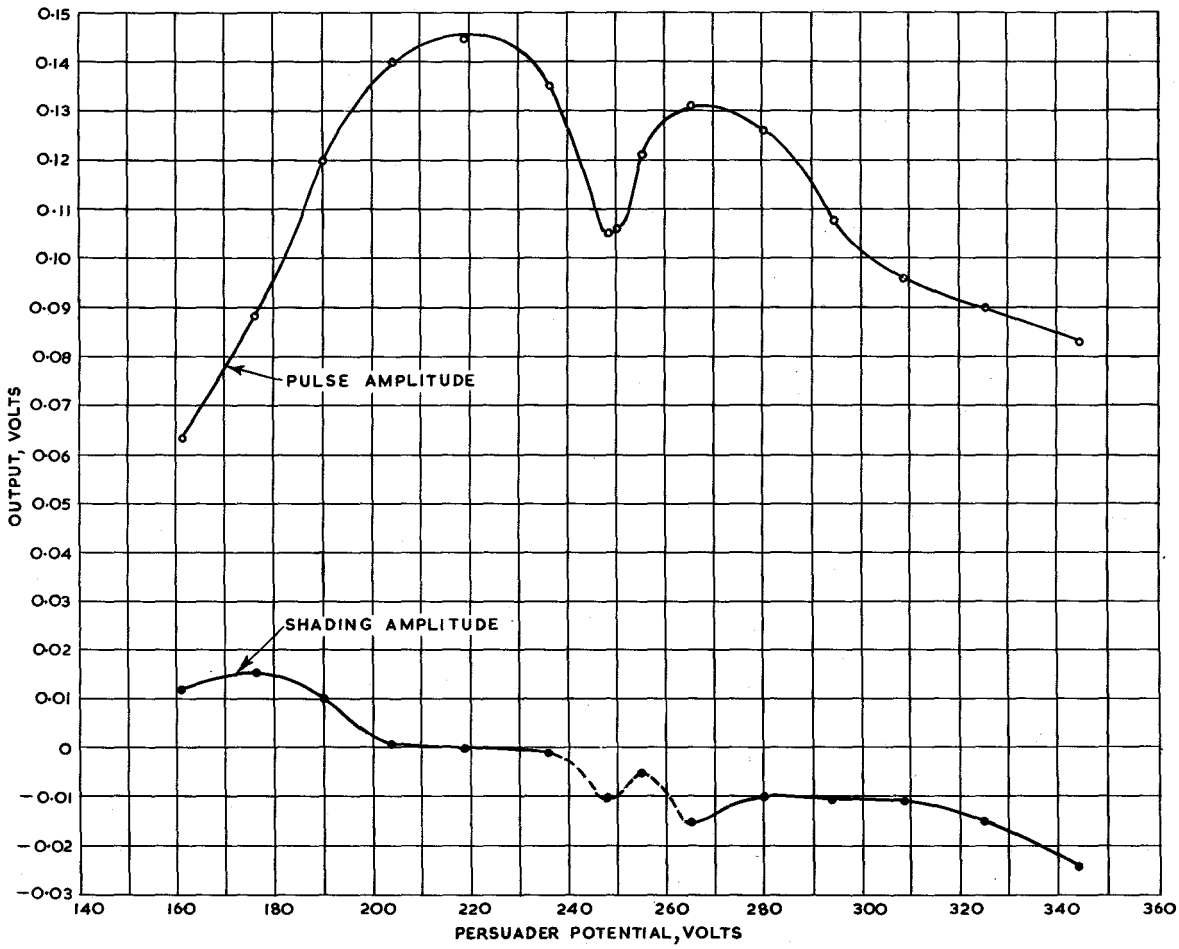

Fig. 7 - The effect of variation of multiplier focus

the results of Section 5 the beam current was determined. The proportion of the beam absorbed by the field mesh was also known from previous measurements (Section 6), thus enabling the beam current returning to D1 to be calculated. The amplitude of the pulse output from the head amplifier was measured and, knowing the tube anode load resistance and the gain of the head amplifier, the tube output current could be calculated. The gain of the multiplier may be defined as the ratio of the tube output current to the return beam current.

The operating conditions under which the measurement was made were as follows. (All voltages are quoted with respect to cathode potential):

Target mesh:	−3·0 V
Decelerator:	−100 V
Wall anode:	+110 V
Field mesh:	+125 V
Persuader:	+220 V

Dynode 1:	+220 V
Dynode 2:	+630 V
Dynode 3:	+820 V
Dynode 4:	+1·0 kV
Dynode 5:	+1·16 kV
Anode:	+1·2 kV
Load resistor (R_L):	12 kΩ
Head amplifier gain (M):	0·73
Field mesh transmission (T):	0·70

Let the *peak* output current of the tube be I_O and the *peak* output voltage of the head amplifier be V_S.

Then $I_O = V_S/(M \times R_L)$

$= 1{\cdot}14 \cdot 10^{-4} \cdot V_S$

Let the *peak* return beam current be I_R so that the multiplier gain is I_O/I_R.

Also let the *mean* field mesh current be I_F and the *mean* outgoing beam current be I_B.

Then $I_R = \frac{100}{94}(I_B - I_F)$

$= \frac{100}{94} I_B T^2$

$= 0{\cdot}521\ I_B$

The factor 100/94 in the above expression is a correction to allow for the fact that the beam current was cut off for 6% of the time, owing to the presence of the pulse.

Table 8 shows the result of these measurements.

TABLE 8

MEASUREMENT OF MULTIPLIER GAIN

Cathode current μA	Mean beam current (I_B) μA	Return beam current (I_R) μA	Pulse amplitude at head amplifier output (V_S) V	Tube output current (I_O) μA	Multiplier current gain
0					
5·0	0·020	0·0104	0·071	8·1	780
7·5	0·030	0·0156	0·115	13·1	841
10·0	0·041	0·0214	0·150	17·1	801
12·5	0·050	0·0261	0·180	20·6	790
15·0	0·059	0·0308	0·220	25·1	816
17·5	0·066	0·0344	0·245	28·0	815
20·0	0·074	0·0386	0·270	30·8	799
22·5	0·081	0·0422	0·30	34·2	811
25·0	0·088	0·0459	0·32	35·6	777
30·0	0·103	0·0537	0·37	41·7	777
40·0	0·129	0·0673	0·44	50·3	748
50·0	0·155	0·0808	0·52	59·4	736

Average multiplier current gain = 791

9.2. The Second Method Used to Determine Multiplier Gain

The negative-going pulses were removed from G1, and d.c. microammeters were used to measure the multiplier output current and the cathode current; the field-mesh current was measured with a galvanometer as a check on the previous measurement of the transparency of the field mesh. If the cathode current is known, the beam current can be determined (Section 5). If the field-mesh current is subtracted from the beam current, then the beam current returning to D1 is known. The multiplier gain was again taken as the ratio of the tube output current to the return beam current. The operating conditions of the tube were identical with those used in the previous measurement.

Table 9 shows the results of these measurements.

TABLE 9

MEASUREMENT OF MULTIPLIER GAIN

Cathode current	Field-mesh current (I_F)	Beam current (I_B)	Return beam current ($I_B - I_F$)	Tube output current (I_O)	Multiplier current gain
μA	μA	μA	μA	μA	
0	–	–	–	–	–
5·0	0·01	0·020	0·010	8·1	810
7·5	0·015	0·030	0·015	12·5	835
10·0	0·021	0·041	0·020	16·9	847
15·0	0·030	0·059	0·029	24·3	839
20·0	0·039	0·074	0·035	31·8	909
25·0	0·045	0·088	0·043	36·5	849
30·0	0·053	0·103	0·050	42·0	840
40·0	0·065	0·129	0·064	52·0	813
50·0	0·079	0·155	0·076	61·0	802
60·0	0·091	0·182	0·091	71·0	780
70·0	0·104	0·209	0·105	78·0	742
80·0	0·116	0·235	0·119	87·0	731
90·0	0·131	0·265	0·134	95·0	709
100·0	0·145	0·294	0·149	103·0	691
110·0	0·159	0·32	0·160	110·0	689

Average multiplier current gain = 839 (over the range 0 to 50 μA cathode current)

The results of both methods are plotted graphically in Fig. 8. It will be seen that they are in close agreement and that the input/output characteristic of the multiplier, plotted over a wide range of return beam currents is somewhat non-linear, and this accounts for the fall in output signal amplitude which may be observed when the beam current is greatly increased.

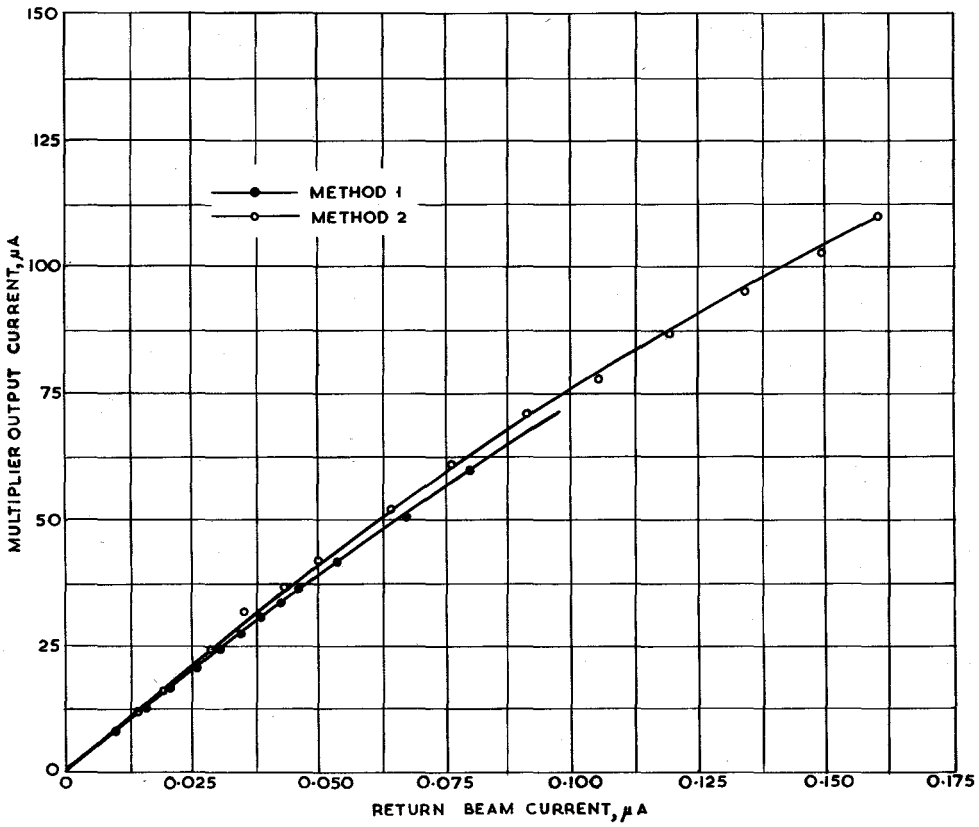

Fig. 8 - Multiplier gain measurement

The useful gain at several return beam currents has been calculated, assuming that the beam returning to D1 is 40% modulated by picture information (see Section 10).

Let i_1 = Maximum return beam current

i_2 = Output current with i_1 returning to D1

i_3 = Output current with 0·6 i_1 returning to D1

Then the useful gain M_U may be defined as

$$M_U = \frac{i_2 - i_3}{0{\cdot}4\ i_1}$$

The calculations have been based upon the second method of measurement; they are given in Table 10.

TABLE 10

VARIATION OF USEFUL GAIN OF MULTIPLIER AS A FUNCTION OF RETURN BEAM CURRENT

Maximum return beam current (i_1)	Multiplier output current at maximum return beam current (i_2)	Multiplier output current at 60% of maximum return beam current (i_3)	Change in multiplier output current	40% of maximum return beam current	Useful gain
μA	μA	μA	μA	μA	
0·03	25	15	10	0·012	833
0·06	48	30	18	0·024	750
0·08	63	39	24	0·032	750
0·10	76	49	27	0·040	675
0·12	88	57	31	0·048	646
0·15	105	69	36	0·060	600

These results are shown graphically in Fig. 9.

From these results it may be concluded that the multiplier gain cannot be regarded as a fixed figure, but will vary as the return beam current is changed. This implies that the effective multiplier gain will vary with the exposure and target mesh potential, since both these factors affect the amount of beam required to discharge the target and hence the magnitude of the return beam. Furthermore, the use of excessive beam current will reduce the gain and therefore reduce the output signal.

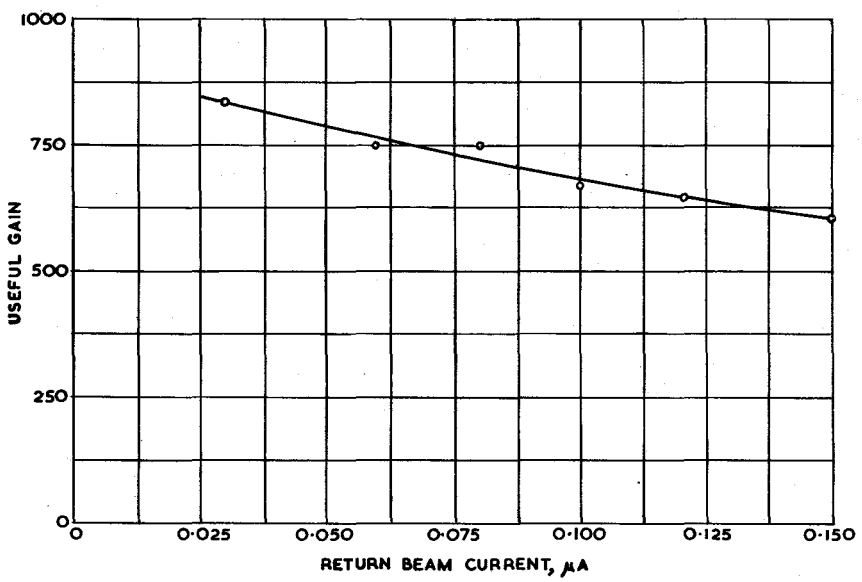

Fig. 9 - The variation of useful gain as a function of beam current

10. THE MEASUREMENT OF THE DEPTH OF MODULATION OF THE RETURN BEAM

When the electron beam of the tube scans the target, electrons are collected by the target in accordance with the positive charge pattern produced by the image section. On the one hand, the beam current must be high enough to discharge the areas of the target corresponding with peak white; on the other hand, it must not be made too large or the noise level will be raised and the amplification of the electron multiplier will be reduced (see Section 9). It has been found that the target cannot absorb all the beam current, even at points corresponding to maximum scene brightness. The main reasons appear to be:

(i) The beam contains electrons with differing velocities of emission from the cathode. As an elementary area of the target receives charge from the beam, its potential falls and only the faster electrons are able to land.

(ii) Secondary emission from the scanned side of the target prevents complete absorption of the beam by the target.

(iii) The scanning spot is not of uniform density, and its edge is not sharply defined. During its movement across the target the spot will overlap the area already partially discharged during the previous line of the same field, and also the rear edge of the spot will be covering that part of the target already subjected to the action of the more dense centre of the scanning spot.

When making measurements of beam modulation depth, the choice of "peak white" at which the measurement is made presents some difficulty. The results depend not only upon the brightness of the scene but also on the size of the bright area taken as "peak white" and the brightness of other parts of the scene.[3] Measurements were made using the B.B.C. Test Transparency 51[4] and a line passing through the step wedge was selected.

During the measurements the tube was operated normally, except that a line scan frequency negative-going pulse was applied to G1 (as in "The Measurement of Gain of the Multiplier Section", Section 9) and an oscilloscope was used to examine the head amplifier output. The cathode current was raised to about 70 μA and the lens iris opened until the channel was operating half a stop above the "knee", this setting being judged by the oscilloscope waveform (see Fig. 10, in which the steps of the wedge and the large positive-going pulse, caused by the cutting off of beam current by the keying waveform on G1, can be seen). The waveform amplitudes corresponding to the "peak white" of the wedge and to beam current cut off were recorded. The beam current was progressively reduced and the waveform amplitudes measured for several values of cathode current. A series of measurements was made for each of three values of target mesh potential. The results are given in Table 11 and are shown in graphical form in Fig. 11.

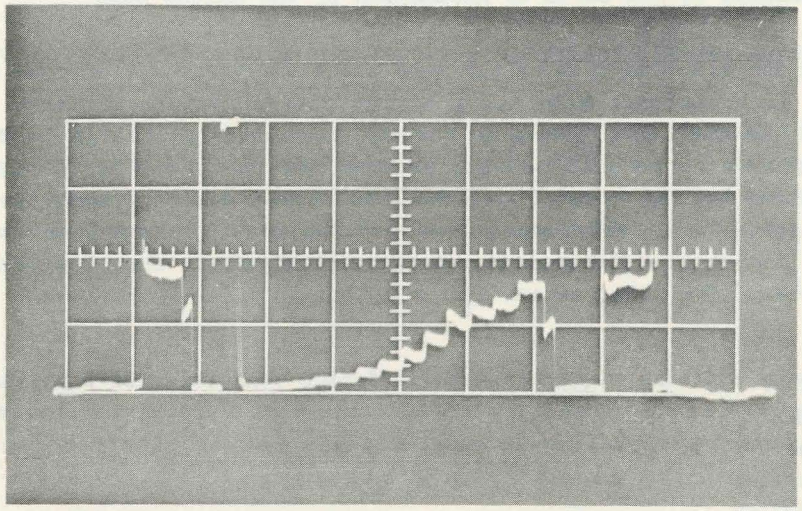

Fig. 10 - Depth of modulation measurement

Oscilloscope trace showing grey scale wedge representing the total signal excursion and the pulse representing 100% modulation by cut-off of the beam

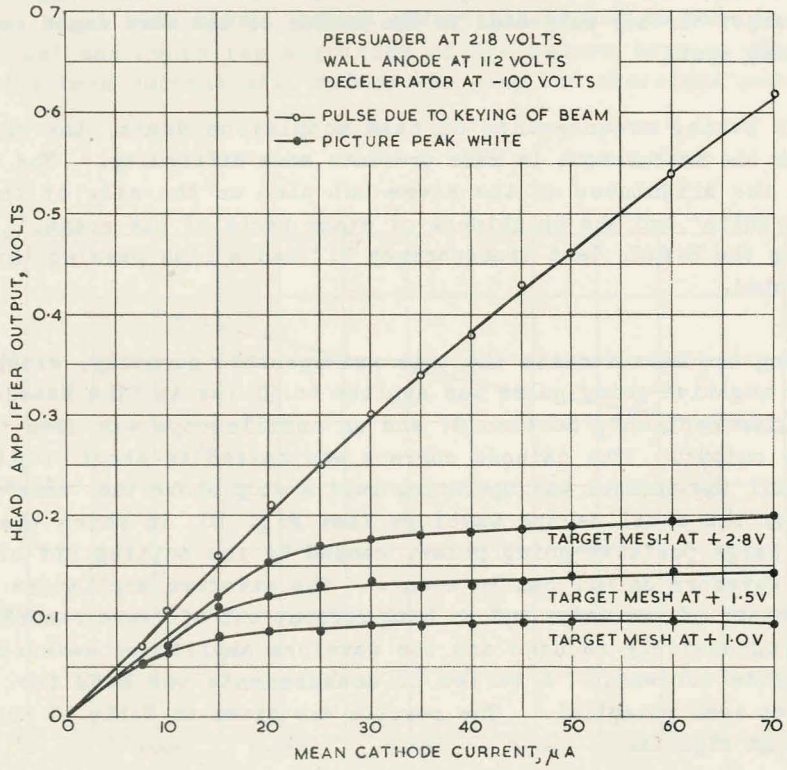

Fig. 11 - The depth of modulation of the return beam

TABLE 11

BEAM MODULATION DEPTH

Cathode current	Target mesh = −1·0 V (i.e. +1·0 V above cut off)		Target mesh = −0·5 V (i.e. +1·5 V above cut off)		Target mesh = +0·8 V (i.e. +2·8 V above cut off)	
	Pulse amplitude	Peak-white amplitude	Pulse amplitude	Peak-white amplitude	Pulse amplitude	Peak-white amplitude
μA	V	V	V	V	V	V
7·5	0·07	0·055*	0·07	0·05‡	0·07	0·04‡
10	0·105	0·065*	0·10	0·08†	0·11	0·07‡
15	0·16	0·080	0·16	0·115	0·17	0·12‡
20	0·21	0·085	0·21	0·12	0·22	0·155†
25	0·25	0·085	0·23	0·13	0·27	0·170
30	0·30	0·090	0·29	0·135	0·315	0·175
35	0·34	0·090	0·34	0·13	0·355	0·180
40	0·38	0·090	0·36	0·13	0·39	0·185
45	0·43	0·095	0·40	0·135	0·44	0·185
50	0·46	0·095	0·46	0·14	0·47	0·190
60	0·54	0·095	0·56	0·145	0·56	0·195
70	0·58	0·09	0·59	0·14	0·62	0·20

* Top step just visible

† Top step missing

‡ "Fold-over" of top step.

These measurements show that, as the cathode current is increased, the signal output from the tube gradually approaches a limiting value which depends on the target mesh potential. Changes in cathode current then make little difference to signal amplitude, but they have a direct effect on the total beam and therefore on the depth of modulation and the signal-to-noise ratio. With low values of cathode current, the top steps of the wedge were either flattened or, under some conditions, reversed. In order to standardize the results, the cathode current at which the modulation depth was measured was taken, arbitrarily, as that current for which the amplitude of the signal due to the white rectangle of the step wedge of Test Card 51 was 95% of maximum; the pulse amplitude, V_P, corresponding to the interruption of this current was measured, and the percentage modulation taken as:

$$\frac{0{\cdot}95\ V_{P.W.}}{V_P}$$

where $V_{P.W.}$ = The maximum output voltage corresponding to peak white in the scene.

TABLE 12

DEPTH OF MODULATION

Target mesh potential above cut-off	Waveform amplitude, peak white	0·95 of peak white	Cathode current when output is 0·95 of peak white	Pulse amplitude	Modulation
V	V	V	μA	V	%
+1·0	0·09	0·0855	23	0·215	40
+1·5	0·142	0·135	35	0·34	39·5
+2·8	0·20	0·19	55	0·50	38

These results are more consistent than might have been expected, the main difficulty being to decide on the cathode current at which to measure the pulse due to the total beam. There is inevitably some scatter in the points given by the peak-white signal measurements, so the drawing of smooth curves among them is to some extent a matter of opinion; a small change in the curve can make a large change in the cathode current at which the output is taken to be 0·95 of maximum.

The depth of modulation found by this method is not strictly the figure for the return beam since it includes the non-linearity of the electron multiplier. However, in view of the possible errors in these measurements it would be pointless to correct the results for this non-linearity. The measurements indicate a modulation depth of 40%; this result is in conformity with the figure of 30% to 40% quoted by Pilz.[2]

11. MEASUREMENT OF CURRENTS IN THE IMAGE SECTION

This series of measurements was devised to examine the following aspects of the image section:

(i) the sensitivity of the photocathode.

(ii) the contribution of the image section to the "knee" of the transfer characteristic.

(iii) the secondary emission coefficient of the target.

In each case the camera channel was set up normally and focused on an area of uniform brightness. Mirror galvanometers were connected in series with the photocathode and target mesh leads. Small currents found to flow through the galvanometers when the lens was capped were caused by leakage through the insulation of the tube and its connections; these leakage currents were only slightly reduced when the tube was removed from the yoke. The currents resulting from photo-emission were taken as those indicated by the changes in galvanometer deflections when the lens was capped and uncapped. The illumination of the photocathode was varied partly by changing the brightness of the light source, but mainly by using the calibrated iris of the lens.

The illumination was calculated from the formula

$$I = \frac{T_L B}{4f^2(1 + m)^2}$$

where I = photocathode illumination (lumens/sq ft)

B = scene brightness (ft-lamberts)

f = relative aperture

T_L = lens transmission, assumed to be 80%

m = optical magnification, in this case 0·11

Inserting the values of T_L and m gives

$$I = 0{\cdot}162 \frac{B}{f^2}$$

11.1. The Sensitivity of the Photocathode

The photocathode current was measured at various illumination levels. The results are given in Table 13 and are shown graphically by curve d in Fig. 12.

The electrode potentials were as follows:

Photocathode: −400 V

Target mesh: +2 V with respect to cut off

TABLE 13

PHOTOCATHODE SENSITIVITY

Scene brightness (B) ft-L	Relative lens aperture (f)	Photocathode illumination (I) lm/sq ft	Photocathode current (i_{pc}) μA
30	5·6	0·155	0·054
30	8	0·076	0·028
30	11	0·040	0·016
30	16	0·019	0·0088
30	22	0·010	0·0035

The dimensions of the area of the photocathode used were 1·28 in × 0·96 in (3·25 cm × 2·44 cm). The luminous flux on the target is, therefore,

$$F = 0{\cdot}00854\ I \text{ lumens}$$

From the photocathode current graph in Fig. 12

$$i_{pc} = 0{\cdot}36\ I$$

The photocathode sensitivity is therefore 42 μA/lumen. This figure is well within the manufacturer's tolerance.

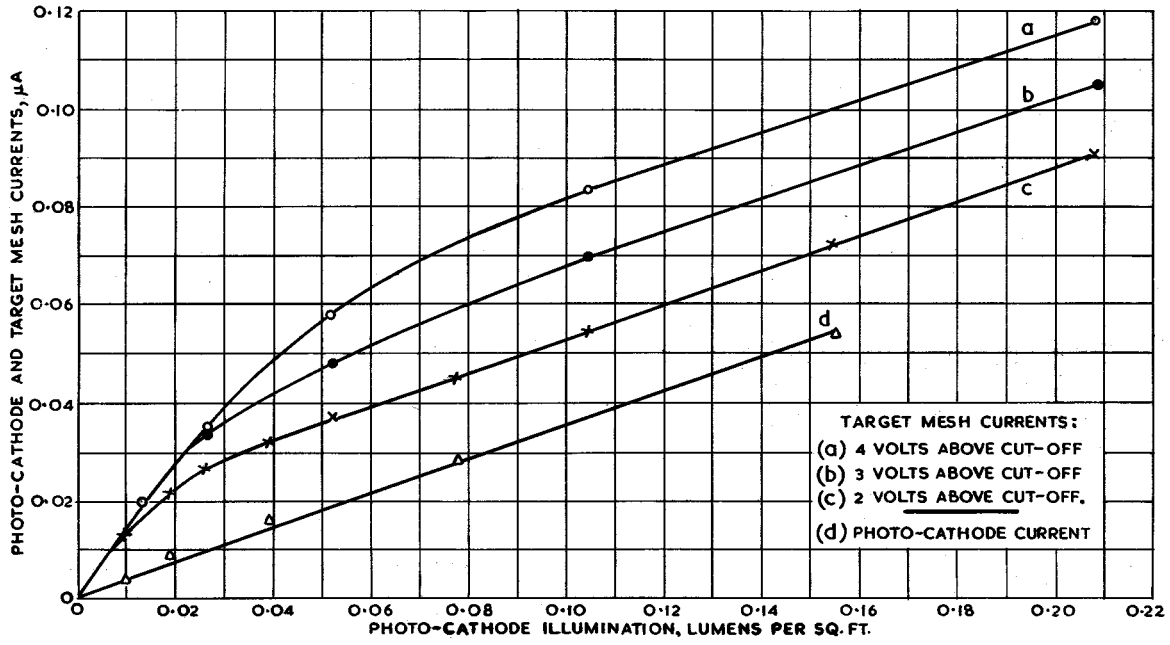

Fig. 12 - Currents in the image section

11.2. The Contribution from the Image Section to the "Knee" of the Transfer Characteristic

In order to investigate the production of the "knee" of the transfer characteristic, a series of measurements was made of the target mesh current as a function of the photocathode illumination at various settings of the target mesh potential V_{TM}, given below in volts above cut off.

The results are given in Table 14 and shown graphically by curves a, b and c in Fig. 12.

TABLE 14

TARGET MESH CURRENTS

Photocathode illumination lm/sq ft	Target mesh current V_{TM} = +2 V μA	V_{TM} = +3 V μA	V_{TM} = +4 V μA
0·010	0·0135	–	–
0·013	–	–	0·020
0·019	0·0215	–	–
0·026	0·027	0·033	0·035
0·039	0·032	–	–
0·052	0·037	0·048	0·058
0·078	0·045	–	–
0·104	0·054	0·070	0·083
0·155	0·0725	–	–
0·208	0·091	0·105	0·118

It will be seen from the curves of Fig. 12 that as the target mesh voltage is raised, the "knee" of the curve is less sharp and occurs at a higher level of illumination.

11.3. The Secondary Emission Coefficient of the Target

From the results of the measurements of Section 11.1. it will be seen that the photocathode current is closely proportional to the illumination. We can therefore write $i_{p_c} = KI$; where K is a constant representing the sensitivity of the photocathode (in this case 0·36, as found in Section 11.1.). If the transparency of the target mesh is assumed to be 0·7 the primary current to the target is 0·7 KI and that to the mesh is 0·3 KI.

Let the secondary emission ratio of the target be S. Consider the tube to be operating below the "knee" of the transfer characteristic so that the secondary emission from the target is $0{\cdot}7KIS$.

The total mesh current is then $0{\cdot}7KIS + 0{\cdot}3KI = (0{\cdot}7S + 0{\cdot}3)\,KI$.

The initial slope of the graph of target mesh current against illumination, when operating below the "knee", is therefore $(0{\cdot}7S + 0{\cdot}3)K$.

Above the "knee", the effective secondary-emission ratio of the target is unity, so that the slope of the graph becomes K; by finding the ratio of these slopes we can, therefore, determine S. As a check, it will be seen that the slope of the target mesh current curve above the "knee" is the same as the slope of the photocathode current graph, indicating that no further contribution to the target mesh current is being made by secondary emission from the target.

The initial slopes of the target mesh current curves in Fig. 12 are approximately 1·5.

The final slope of these curves is approximately 0·36, therefore we may write:

$$\frac{(0{\cdot}7S + 0{\cdot}3)K}{K} = \frac{1{\cdot}5}{0{\cdot}36}$$

$$\therefore\ S = 5{\cdot}5$$

This figure is of the same order as the figure 4 to 5 mentioned by A.A. Rotow.[5]

12. CONCLUSIONS

This report has described in some detail a number of measurements made to establish the magnitudes of various current-flows within the 4½ in image orthicon and some interesting facts have been revealed. From the cathode current produced by the electron gun only about one third of one per cent emerges from the minute aperture in the anode to form the scanning beam and thirty per cent of that strikes the field mesh on its outward journey towards the target. The return beam has become less

than 40% modulated with signal information and this receives amplification of about 800 times in the electron multiplier section to become a signal output current of about fifteen microamperes.

It has been established that the operational expedient of adjusting the persuader electrode for maximum output signal to give an approximate coincidence with minimum shading conditions is valid provided the one correct maximum out of several possibles has been selected. It has also been found that the field mesh will produce undesirable secondary emission if its potential is allowed to fall to less than 15 volts in excess of that of the wall anode.

On the image side of the target, photocathode sensitivity is found to be about 40 μA per lumen and the current is linearly related to illumination over the normal working range. The secondary emission ratio of the target, when working below the knee, is approximately 5·5 to 1.

These results are those of only one particular tube but they are nevertheless believed to be typical values.

13. REFERENCES

1. Brothers, D.C., "The Testing and Operation of 4½ in Image Orthicon Tubes", J.Brit.I.R.E., Vol. 19, No. 12, December 1959, pp. 777-805.

2. Pilz, F., "Procedures for Testing and Measuring Characteristics of Image Orthicon Tubes", Rundfunktechnische Mitteilungen, Vol. 1, No. 4, 1957, pp. 125-138.

3. "Image Orthicon Investigations: The Local Effects of Small-Area Highlights", Research Department Report No. T-100/2 (in preparation).

4. Hersee, G., and Royle, J.R.T., "Two New B.B.C. Transparencies for Testing Television Camera Channels", B.B.C. Engineering Division Monograph No. 21, November 1958.

5. Rotow, A.A., "Image Orthicon for Pickup at Low Light Levels", R.C.A. Review, Vol. 17, No. 3, September 1956, pp. 425-435.

BRH

Printed by B.B.C. Research Department, Kingswood Warren, Tadworth, Surrey